RESEARCH PAPER

Effect of Aging Process on Microstructure Evolution and Mechanical Properties of UFG Zn-22Al Alloy

Bahram Azad, Ali Reza Eivani*, Mohammad Taghi Salehi

* aeivani@iust.ac.ir

School of Metallurgy and Materials Engineering, Iran University of Science and Technology (IUST), Tehran, Iran

Abstract: *Microstructure evolution and mechanical properties of Zn-22Al alloy after post-ECAP natural/artificial ageing were investigated. A homogenization treatment was applied to the casting samples. In addition, after preparing the samples for the ECAP, secondary homogenization treatment was done and then the samples were quenched in the water to form a fine-grain structure. After 8 passes of ECAP, some ECAPed samples were naturally aged and some ECAPed samples were artificially aged. Natural ageing after 8 passes of ECAP showed that Zn-22Al alloy has a quasi-stable microstructure because limited grain growth occurred. The two-phase structure of Zn-22Al alloy prevented excessive grain growth after natural ageing. On the other hand, artificial ageing after 8 passes of ECAP caused relatively much grain growth to take place. In shorter times of artificial ageing, the grain growth rate is faster due to the high surface energy of grain boundaries. On the contrary, as the time of artificial ageing increased, the surface energy of grain boundaries decreased, which led to a decrease in the grain growth rate. In addition, texture evolution was studied after ageing artificially. Therefore, the main texture of α and η phases was determined.*

Keywords: Zn-22Al alloy, ECAP, Natural ageing, Artificial ageing, Superplasticity.

1. INTRODUCTION

Zn-22Al eutectoid alloy has a high theoretical and practical value among the group of Zn-Al alloys [1-3]. One of the valuable features of Zn-22Al alloy is having superplastic behaviour at room temperature [1-3]. Superplastic materials are polycrystalline solids that can withstand large uniform deformation before failure [4]. The most important characteristic of a superplastic material is its high strain rate sensitivity (m) which is expressed as Eq. (1):

$$\sigma = k \, \dot{\varepsilon}^{m}, \qquad \text{Eq. (1)}$$

In this equation, σ, ε and k are the deformation stress, the strain rate and the constant of the material [4]. For superplastic behaviour, the value of m should be equal to or greater than 0.3, while for the majority of superplastic materials, the value of m has been reported between 0.4 and 0.8 [4]. When a sample with high m is subjected to uniaxial tension, the presence of a neck causes the local strain rate to increase and also the flow stress rapidly increases in the neck region [4]. As a result, this neck is subjected to the strain rate hardening and this situation prevents the neck from further growth. High m causes the test sample to have a high resistance against the neck growth which results in high elongation to failure (e_f) in the sample [4].

The most important mechanism of superplastic deformation is grain boundary sliding [1, 5]. The behaviour of superplastic materials is very sensitive to the test temperature and grain size [1, 2, 4]. The first basic requirement for superplastic behaviour in a material is the presence of very fine grains [1, 4]. Hence, it is important to understand the fundamental metallurgical principles of grain refinement and grain growth. It is important to note that only obtaining a fine-grained structure is not sufficient to exhibit superplastic behaviour because it is necessary to keep the grain size stable during deformation [6]. Achieving a fine-grained structure leads to an increase in workability in superplastic deformation. To achieve superplastic behaviour, a grain size of less than 10 μm is required [7]. Indeed, the metal must be deformed at high temperatures (above 0.5 T_m) and low strain rates (between 10^{-5} s^{-1} to 10^{-3} s^{-1}) [8]. It should be noted that superplastic behaviour can occur at lower temperatures and higher strain rates, which requires that the grain size of the material becomes smaller [1, 8]. Recent studies have shown that even room-temperature superplastic behaviour occurs if the grain size reaches sub-micron levels [1-3, 8]. Equal channel angular pressing (ECAP) is one of the severe plastic deformation (SPD) techniques to achieve metals with very fine grains [1].

Therefore, in many superplasticity studies of Zn-22Al alloy, the ECAP process has been used to achieve an ultrafine-grained (UFG) structure [1, 3, 8].

Zn-22Al alloy is considered a seismic damper [9]. Therefore, considering such an application for Zn-22Al alloy, the stability of the microstructure and maintaining the superplastic behaviour are important parameters, because any excessive grain growth can harm the superplastic behavior of the Zn-22Al alloy [10]. Considering Zn-22Al alloy showing superplastic behaviour at room temperature, the microstructure stability of the alloy during storage at room temperature is important, because the room temperature is almost equal to half of the melting point of Zn-22Al [2, 8]. Therefore, it is important to study the microstructure evolution and mechanical properties of Zn-22Al alloy after natural and artificial ageing. Previous studies have shown that natural ageing causes grain growth and subsequently, harms the grain boundary characteristics of Zn-Al alloys [2, 8]. There are limited studies of the effect of natural ageing (also known as natural annealing) on the superplastic behaviour of Zn-Al alloys [2, 8]. Demirtas et al [8] reported that the natural ageing of Zn-22Al alloy at room temperature leads to a decrease in e_f and the maximum of e_f occurs at lower strain rates. Savaşkan et al [10] reported that the ageing of Zn-Al-Cu alloy at 200°C for 2 hours causes the formation of a mixed structure of fine and equiaxed grains and cellular material. Another study showed that the microstructure of Zn-22Al alloy after aging at 250°C for 30 min contains very fine equiaxed grains [11].

Microstructure stability during a tensile test or isothermal storage such as aging is an important factor in investigating superplastic behavior and mechanical properties of superplastic materials. Considering the melting point of Zn-22Al alloy, room temperature is approximately half of the melting point of this alloy, which means that grain growth is expected to occur at room temperature after grain refinement. Therefore, investigating the effect of long-term natural ageing on the microstructure and room temperature superplastic behaviour of UFG Zn-22Al alloy seems necessary for some applications such as seismic damper, which was studied in this research. Also, another aim of the current article is to study artificial ageing and achieve a microstructure with different grain sizes and its effect on the microstructure and mechanical properties of Zn-22Al alloy.

2. EXPERIMENTAL PROCEDURES

An induction furnace was used to produce the Zn-2Al alloy. The chemical composition of the obtained alloy is given in Table 1. The samples were homogenized at 375°C for 24 h after casting. Then, ECAP samples with 130 mm in length and 15.8 mm in diameter were prepared. The prepared ECAP samples were subjected to secondary homogenization heat treatment at 375°C for 48 h. Then, the samples were quenched in water to form a fine-grain structure. The inner surface of the mold channels and the sample surface were completely coated with MoS_2 lubricant. The ECAP was performed at room temperature and up to 8 passes using the B_C route. Zn-22Al alloy was subjected to natural ageing at room temperature after 8 passes of ECAP in different time intervals between 30 and 480 days. Also, some ECAP samples were subjected to artificial ageing at different temperatures and times to produce different microstructures.

Scanning electron microscope (SEM)-TESCAN Vega was used to study the microstructure of the samples. The samples prepared to study the microstructure were cut at least 10 mm from the end of the sample so that the oxide layer did not play a role in the analysis. The samples were sanded first and then polished by spraying a solution of water and alumina until they reached a completely mirror-like surface. After polishing, the samples were etched in a solution containing 5 g of CrO_3, 0.25 g of Na_2SO_4, and 100 ml of H_2O and then studied by SEM. Texture evolution was characterized by electron backscattering diffraction (EBSD) in a scanning electron microscope with a field emission type gun (FE-SEM; Philips XL30) operated at 15 kV and a transmission electron microscope (TEM; Hitachi H-800, Philips CM200 FEG, JEOL JEM2010) operated at 200 kV.

Table 1. The chemical composition of the cast alloy

Element	Mg	Fe	Pb	Sn	Al	Zn
Wt%	0.01	0.001	0.003	0.001	21.87	balance

2

To investigate changes in the strength and ductility of the alloy after the ageing process, a uniaxial tensile test was performed at room temperature and different strain rates. The tensile test samples were prepared on ED-ND plates by wire cutting machine according to ASTM-E8. At each stage, the tensile test was repeated at least three times to obtain accurate results. To evaluate the hardness changes in different stages, the Vickers microhardness test was performed on the samples by the BUEHLER microhardness tester model MMT-7. To obtain the average hardness on the ED-ND plates, the hardness test was repeated eight times for each sample.

3. RESULTS AND DISCUSSION

3.1. Natural Ageing

The TEM image of the microstructure of Zn-22Al alloy after 8 passes of the ECAP at room temperature using the B_C route is shown in Figure 1. As can be seen, ECAP results in a UFG microstructure that consists of well-defined grains with a grain size of about 440 nm. Also, the distribution of Al-rich α phase (light contrast) and Zn-rich η phase (dark contrast) are completely homogeneous throughout the microstructure.
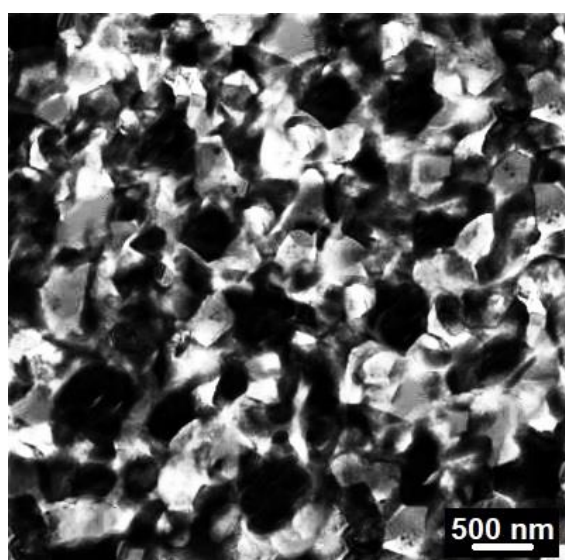

Fig. 1. TEM image of microstructure of Zn-22Al alloy after 8 passes of ECAP at room temperature.

After 8 passes of ECAP, Zn-22Al alloy was subjected to natural ageing in different time intervals between 30 and 480 days. Figure 2 shows SEM images of Zn-22Al alloy aged at room temperature for 30, 120 and 480 days.

Figure 2-a shows that aging after 30 days at room temperature resulted in limited grain growth and the grain size reached about 490 nm. The grain growth after 120 days of ageing (Figure 2-b) is almost small and the grain size reaches about 650 nm. Finally, after 480 days of storage at room temperature (Figure 2-c), the grain size is 780 nm. According to these results, it cannot be said that the UFG microstructure of Zn-22Al alloy is completely stable over time at room temperature after ECAP. However, it can be said that the microstructure is quasi-stable at room temperature after ECAP. After 480 days of storage at room temperature, the grain size increased by about 75% compared to the initial UFG microstructure. The behaviour of Zn-22Al alloy may be related to the eutectoid composition with a two-phase structure. The presence of a secondary phase increases the microstructure stability of superplastic materials during isothermal storage and superplastic deformation [12]. Since Zn-22Al alloy has two phases in its microstructure, they prevent each other from growing and participate in the thermal stability of the alloy. Therefore, it can be said that since Zn-22Al alloy is a two-phase alloy, its grain size is relatively stable at room temperature, which is confirmed by the present study.

True stress-strain curves after the tensile test for natural ageing after 8 passes of ECAP are shown in Figure 3. The results of the stress-strain curve after natural ageing are shown in Figure 4. The values of e_f after 8 passes of ECAP and natural ageing are shown in Figure 4-a. After 8 passes of ECAP, the e_f is about 332% at 10^{-3} s^{-1}. After 30 days of ageing at room temperature, the maximum e_f in Zn-22Al alloy is about 260% at the strain rate of 10^{-4} s^{-1} while in other strain rates, the elongation values decrease. After 120 and 480 days of natural ageing at room temperature, the maximum e_f values are 217% and 172%, respectively, at the strain rate of 10^{-4} s^{-1}. Grain size has a significant effect on the strain rate at which the maximum elongation occurs, and this effect can be expressed as [12]:

$$\dot{\varepsilon} \sim d^{-a}, \tag{1}$$

Where $\dot{\varepsilon}$ is the strain rate at which maximum superplasticity occurs and d is the average grain size. Also, a is a constant value between 2-3. According to this equation, decreasing the grain size leads to an increase in the strain rate where maximum superplasticity occurs. Grain size has a

significant effect on total superplastic deformation. A decrease in grain size leads to an increase in e_f because there is less time for internal voids to grow and maximum elongation occurs at high strain rates [13]. The results obtained in this study are in agreement with the discussions. While a maximum e_f of 332% was obtained at a strain rate of 10^{-3} s^{-1} with size of 440 nm [1], the aged sample with grain size of 780 nm showed a maximum e_f of 189% at a lower strain rate of 10^{-5} s^{-1}.

The changes in the peak true stress with initial strain rate after ECAP [1] and natural ageing are shown in Figure 4-b. A sigma-like behaviour (S shape) that is usually observed in superplastic materials is seen in Figure 4b. It is clear that the stress of Zn-22Al alloy is sensitive to the initial strain rate and an increase in the strain rate leads to an increase in the peak stress finally a peak is seen in Figure 4b, which indicates the highest peak stress. In general, it should be said that at a strain rate of 10^{-1} s^{-1}, which is the highest value of strain rate in this study, the highest peak stress is observed. Comparing the UFG Zn-22Al alloy and the aged Zn-22Al alloy, it is found that this sensitivity prevails for both conditions [1]. The dependence of grain size on stress during the deformation of common polycrystalline materials is expressed by the Hall-Patch equation, in which a decrease in grain size causes an increase in stress [14]. However, during superplastic deformation, GBS is the main deformation mechanism and the transition from conventional deformation to superplastic deformation occurs.
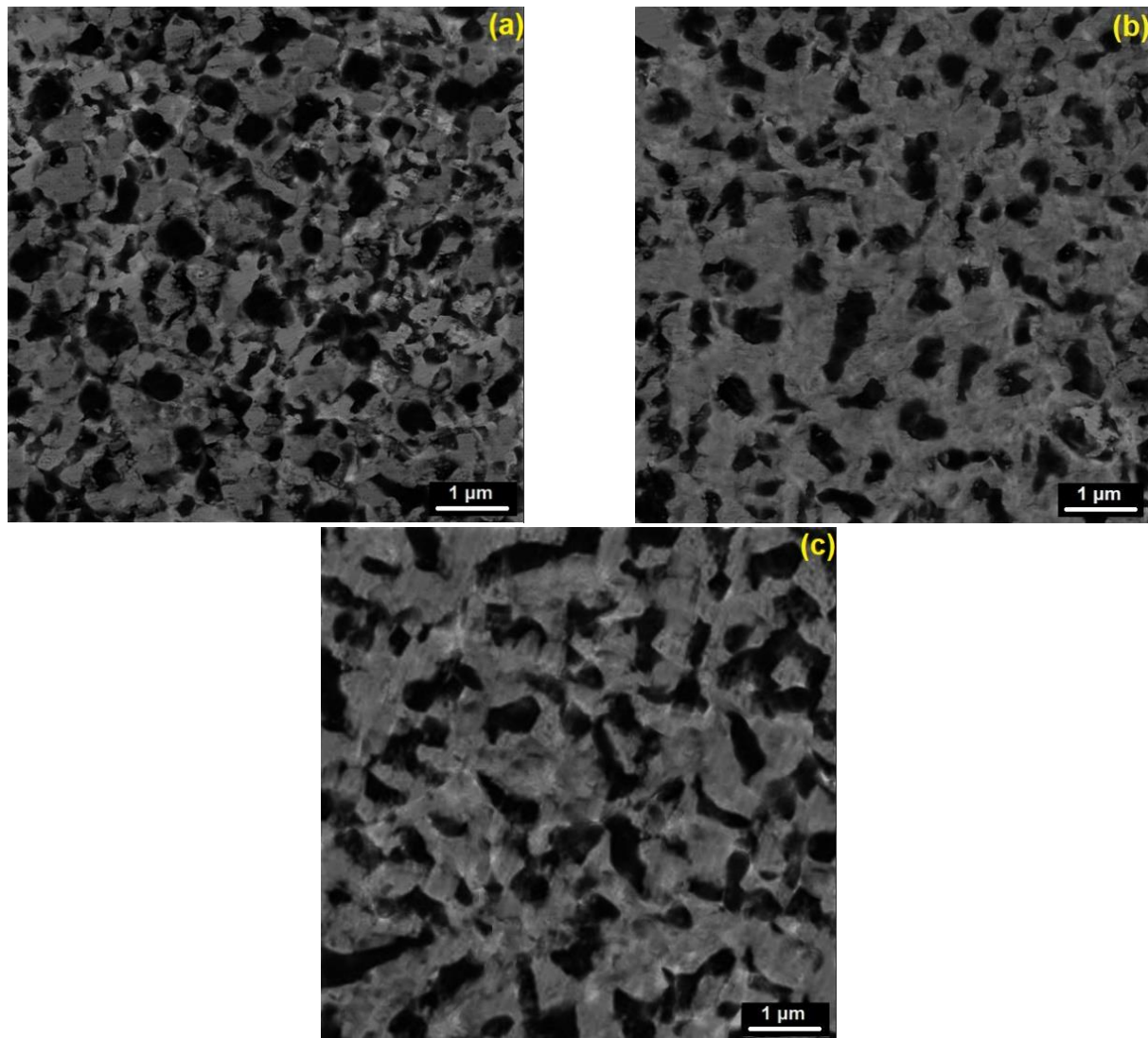

Fig. 2. Microstructure of Zn-22Al alloy aged at room temperature for a) 30, b) 120 and c) 480 days.

In this case, the Hall-Patch relation loses its validity and the dependence of stress on grain size is expressed as [2]:

$$\sigma \sim d^b, \qquad (2)$$

Where σ, d and b are the stress, the grain size and a constant value between 0.7 and 2, which is usually 1, respectively. Therefore, an increase in grain size leads to an increase in stress, which is observed in this study.

It is also necessary to mention that at low strain rates, the tensile test is performed in a longer time compared to higher strain rates, and at room temperature, there is a possibility of DRV, which leads to strain-softening. This strain-softening can be seen as a plateau of the stress-strain curve. At higher strain rates, due to the shorter time of the tensile test, there is not enough time for DRV, and the energy caused by the process can accumulate inside the alloy, and the restoration mechanism appears in the form of DRX. Then, a peak is created in the stress-strain curve and then the stress-strain curve tends downward. Therefore, it can be concluded that the stored energy passes the activation energy barrier and a drop is evident in the curve at a high strain rate. Also, it should be noted that at low strain rates due to the long time of the tensile test, the phenomenon of dynamic softening occurs and a sharp drop is not seen in the stress-strain curve.

The effects of natural ageing on the hardness of UFG Zn-22Al alloy can be seen in Figure 5. The hardness of 8 passes of ECAP is 31 Hv. As seen in this figure, the hardness of the aged Zn-22Al alloy after ECAP increases as the ageing time increases.
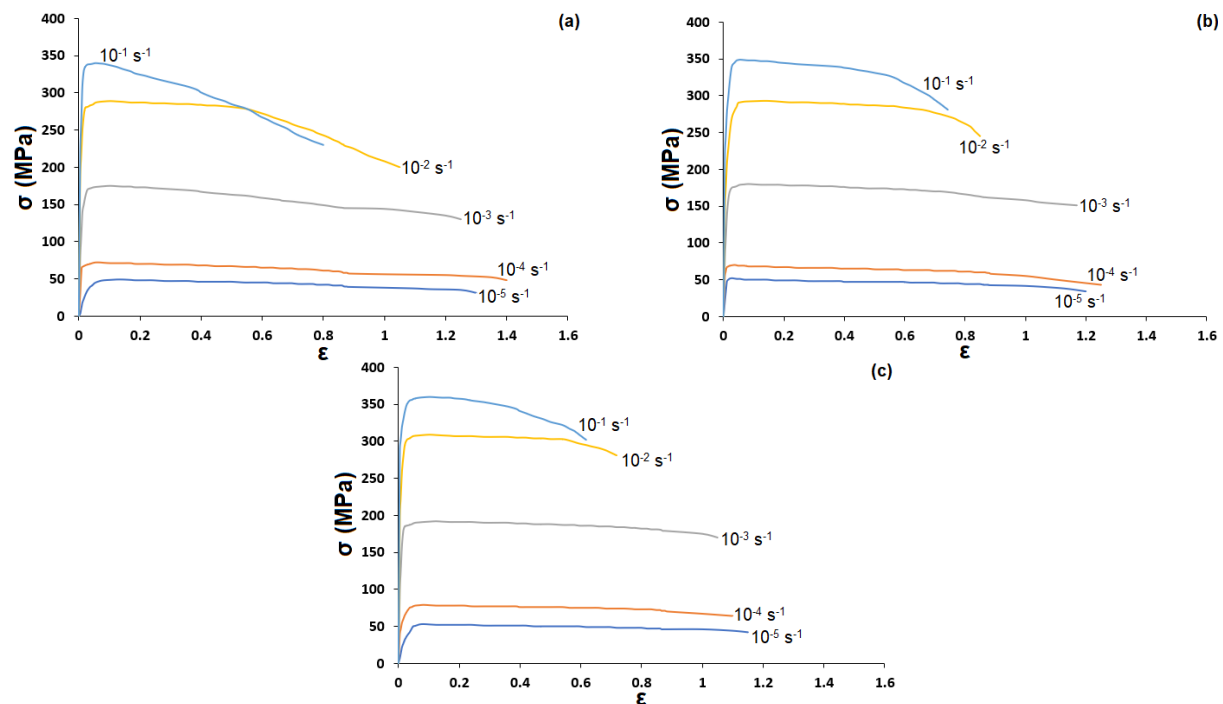

Fig. 3. Stress-strain curves after natural ageing at room temperature for a) 30, b) 120 and c) 480 days.
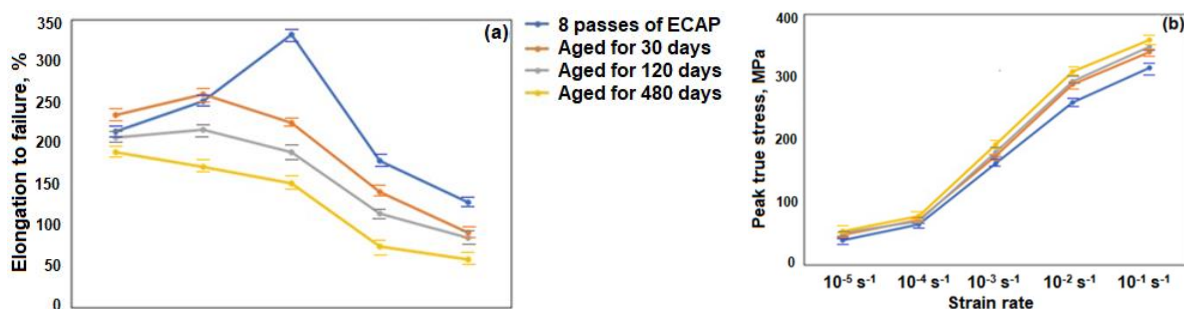

Fig. 4. Changes in a) elongation to failure and b) peak true stress of Zn-22Al alloy after ECAP and natural ageing at room temperature according to initial strain rate.

The hardness of UFG Zn-22Al after 30, 120 and 480 days of natural aging at room temperature is 34, 40 and 42 Hv, respectively. From the relationship between hardness and grain size reported in Figure 2, it is clear that aging-hardening is related to the coarsening of the structure after aging [15]. When the grain size is still small, heat treatment such as natural ageing can harden the alloy by reducing heterogeneous nucleation sites of dynamic recovery/recrystallization (DRV/DRX) [15]. Therefore, after natural ageing, two factors of increasing the grain size and reducing the heterogeneous nucleation site of DRV/DRX cause the hardening of the Zn-22Al alloy.
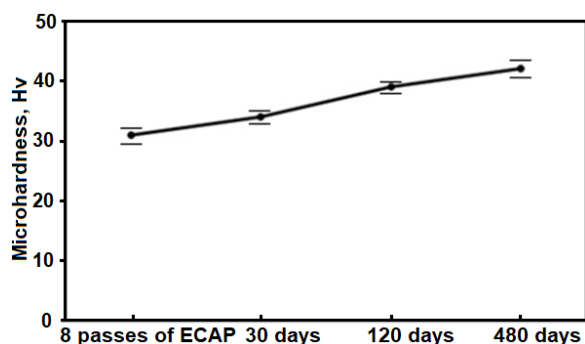

Fig. 5. Microhardness changes of UFG Zn-22Al alloy after natural ageing at room temperature.

3.2. Artificial Aging of Zn-22Al Alloy

In this section, the microstructure and mechanical properties of Zn-22Al alloy after artificial ageing are studied. For this purpose, UFG Zn-22Al alloy was used after 8 passes of ECAP at room temperature. Artificial aging is performed at 100 and 250°C for different times on ECAPed Zn-22Al alloy. SEM images of the microstructure of Zn-22Al alloy in the post-ECAP ageing condition can be seen in Figure 6. The average grain size of the aged samples is calculated from the SEM images by the line intercept technique. The average grain size in each condition is given in Figure 7. The sample after post-ECAP ageing at 100°C and 2 h is called the sample of submicron grain size because only this sample has grain size less than 1 μm after post-ECAP ageing. With increasing ageing time or temperature, more grain growth can be observed after post-ECAP ageing. Shorter ageing times have a higher grain growth rate. As the ageing time increases, the grain growth rate decreases. The mechanism of grain growth in Zn-22Al alloy was studied by Senkov

and Myshlyaev [16]. Grain boundary solute diffusion was proposed as a controlling mechanism for grain growth of Zn-22Al alloy during annealing. Therefore, one of the reasons for the limited grain growth even at the relatively high temperature of 250°C can be the grain boundary solute diffusion that controls the grain boundary migration. Also, from the size of grains obtained at different post-ECAP ageing times, it is clear that the grain growth rate decreases with increasing ageing time, which is due to the change in grain boundary energy level with increasing grain size [17]. The surface energy of grain boundaries increases during the ECAP process due to the formation of UFG microstructure, since smaller grain size means more grain boundary surface area, leading to higher surface energy [18]. In addition, superplastic materials tend to reduce the surface energy of their grain boundaries, which causes the driving force of grain growth [12]. In the early stages of the ageing process, rapid grain growth occurs due to the high surface energy of the grain boundaries. Since increasing the aging time decreases the grain boundary surface energy, the grain growth rate also decreases and a microstructure with higher stability is observed. The present study confirms all the above-mentioned points.

The tensile test behaviour of Zn-22Al alloy after post-ECAP ageing can be seen in Figures 8 and 9. A relatively high strain-softening phenomenon is seen in the sample with sub-micron grain size at all strain rates (Figure 8-a). Also, strain-softening is observed at all strain rates in the sample aged for 8 h at 100°C. However, as the strain rate of the tensile test increases, the strain-softening of this sample decreases (Figure 8-b). For samples aged 32 and 128 h at 100°C (Figures 8-c and 8-d), the strain-softening phenomenon is seen at low strain rates and the strain-hardening phenomenon appears in the curves at high strain rates. After 32 h of ageing at 100°C, strain-hardening appears at strain rates of 10^{-2} s^{-1} and 10^{-1} s^{-1}, and after 128 h of ageing at 100°C, strain-hardening at strain rates of 10^{-4} s^{-1} to 10^{-1} s^{-1} can be observed in the curves.

Almost similar results are observed for samples aged at 250°C. After 2 h and 8 h of ageing at 250°C, strain-softening can be observed in all strain rates of the tensile test, and the value of strain-softening decreases with increasing strain rate (Figures 9-a and 9-b).
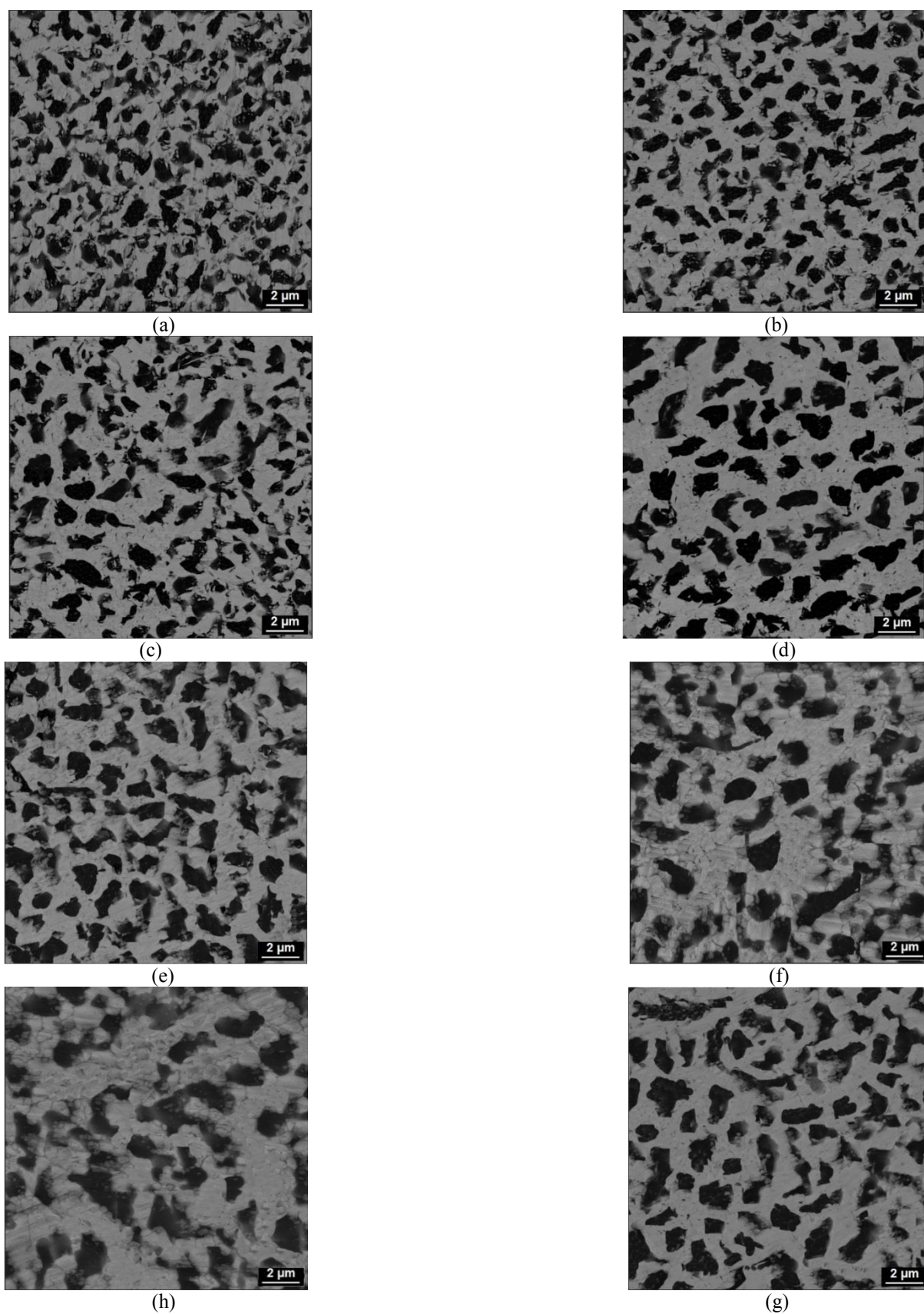
Fig. 6. SEM images of Zn-22Al alloy after post-ECAP ageing at 100°C for (a) 2, (c) 8, (e) 32 and (g) 128 h, at 250°C for (b) 2, (d) 8, (f) 32 and (h) 128 h.
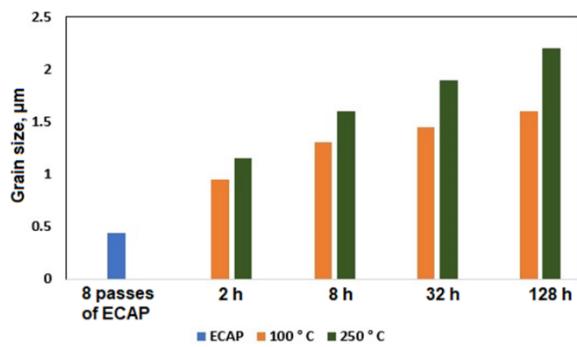
7

Fig. 7. The average grain size of Zn-22Al alloy after post-ECAP ageing at different temperatures and times.

As the ageing time increases, in addition to the strain-softening, the strain-hardening also appears in the stress-strain curves, which can be seen more clearly as the strain rate of the tensile test increases (Figures 9-c and 9-d). As mentioned earlier, the tensile test results of the sample aged at 250°C were similar to the tensile test results of the sample aged at 100°C.

The dependence of strain rate on e_f and peak stress after ECAP and post-ECAP ageing can be seen in Figures 10 and 11. It has been previously reported that the maximum e_f obtained in the sample of 8 passes of ECAP is 332% at a strain rate of 10^{-3} s^{-1} [1]. Also, the e_f was 215%, 252%, 179% and 129% at strain rates of 10^{-5} s^{-1}, 10^{-4} s^{-1}, 10^{-2} s^{-1} and

10^{-1} s^{-1} after 8 passes of ECAP, respectively [1]. The e_f is recorded at 295% and 258% at a strain rate of 10^{-3} s^{-1}, respectively, in 2 h post-ECAP ageing samples at temperatures of 100°C and 250°C (Figures 10-a and 11-a). At less and more than this strain rate and for 2 h of ageing, the e_f decreases. The maximum e_f obtained for the 8h post-ECAP ageing sample at 100°C is 230% at a strain rate of 10^{-4} s^{-1}, for the 32 h and 128 h samples, are 205% and 180% at a strain rate of 10^{-5} s^{-1}, respectively. Also, the maximum e_f of the sample after 8 h post-ECAP ageing at 250°C is 209% at the strain rate of 10^{-4} s^{-1}. For the 32 h and 128 h samples, e_f is 190% and 172% at the strain rate of 10^{-5} s^{-1}, respectively.

Figures 10-b and 11-b show the changes in peak stresses at different strain rates. The peak stress is very sensitive to the strain rate and in all samples, an increase in the strain rate leads to an increase in the peak stress. It is also clear from these figures that grain growth up to 1.28 μm in the 100°C sample and up to 1.15 μm in the 250°C sample causes an increase in the peak stress. An increase in the grain size in these samples, more than the mentioned grain size, leads to a decrease in the peak stress. Therefore, it can be stated that there is a critical grain size any increase in grain size beyond that value will reduce the peak stress.
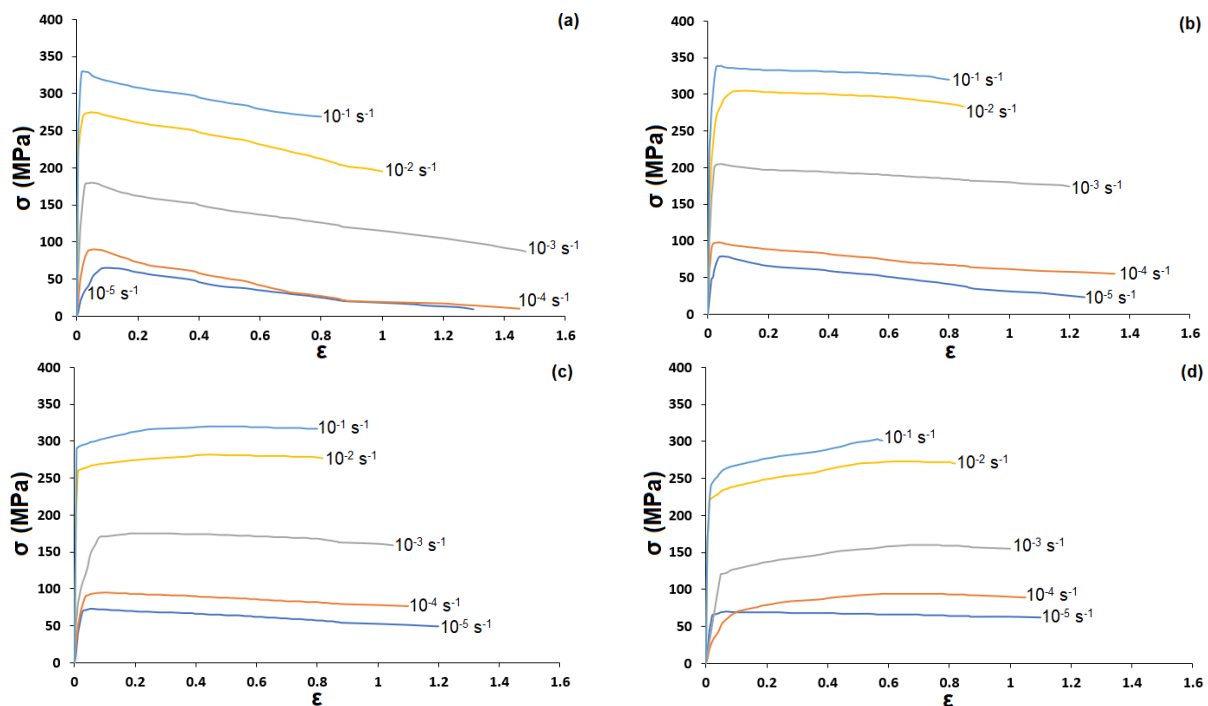

Fig. 8. Stress-strain curves after tensile test in post-ECAP ageing condition at 100°C for (a) 2, (b) 8, (c) 32 and (d) 128 h.
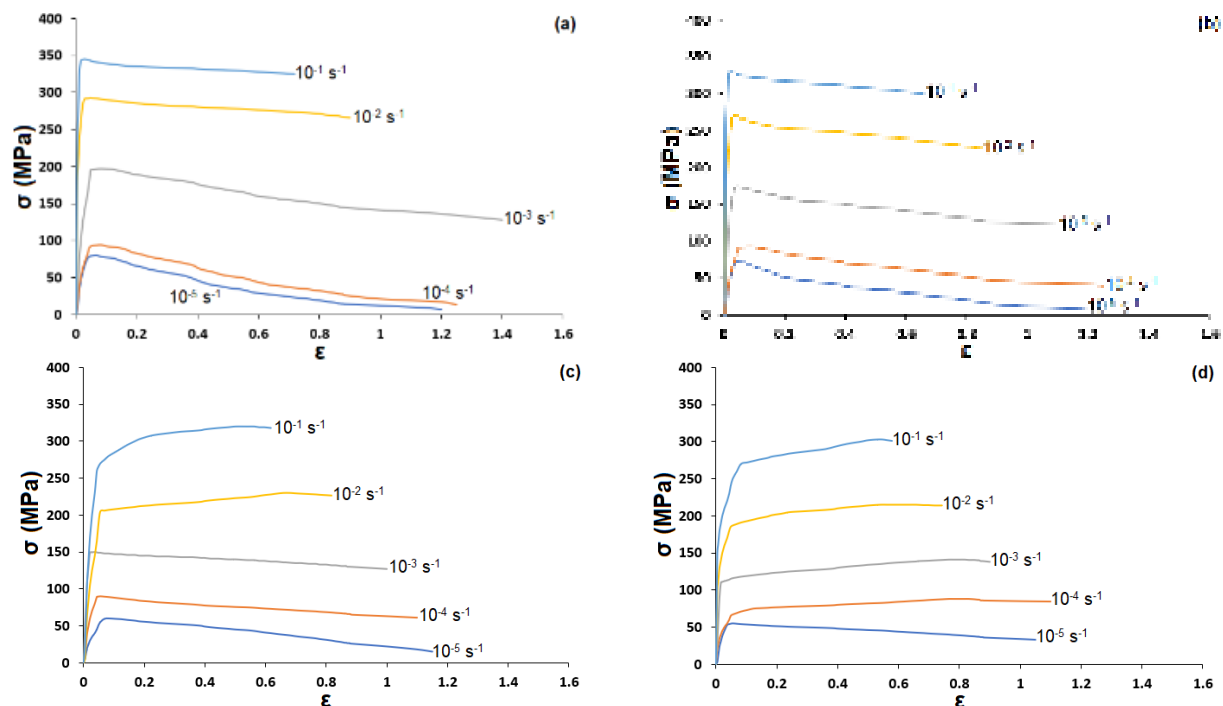
8

Fig. 9. Stress-strain curves after tensile test in post-ECAP ageing condition at 250°C for (a) 2, (b) 8, (c) 32 and (d) 128 h.
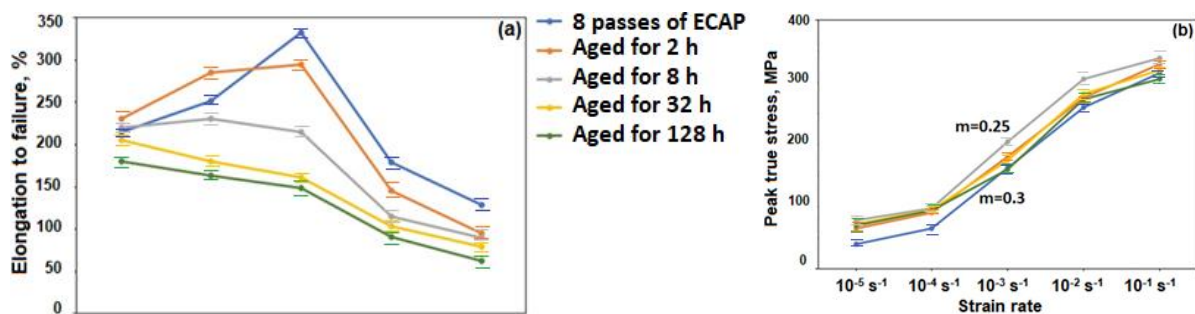

Fig. 10. Dependence of strain rate on a) elongation to failure and b) peak true stress of 8 passes of ECAP and post-ECAP ageing samples at 100°C.
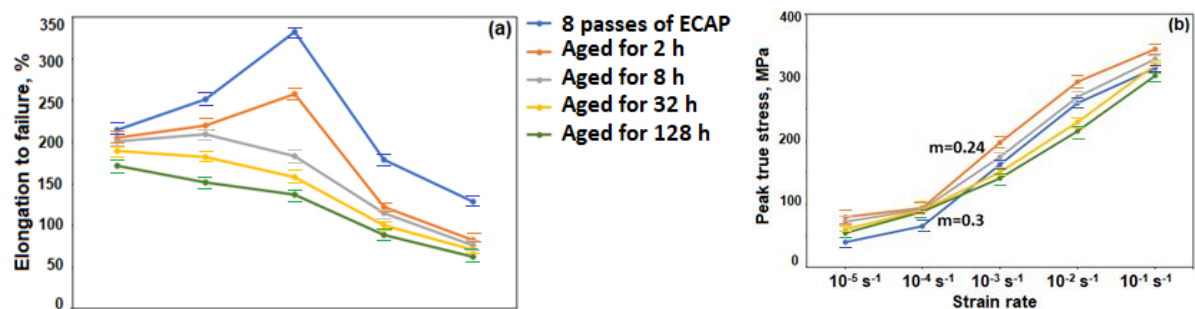

Fig. 11. Dependence of strain rate on a) elongation to failure and b) peak true stress of 8 passes of ECAP and post-ECAP ageing samples at 250°C.

At less than the critical grain size, the transition from the non-superplastic state to the superplastic state occurs [19]. Therefore, decreasing the grain size reduces the stress caused by the easier GBS occurring at higher grain boundaries [19]. The critical grain size is 1.3 μm in this research.

The m value in the region of maximum e_f is about 0.25 and 0.24 for the sample aged 2 h at 100°C and 250°C, respectively. As the ageing time increases, the amount of m decreases. The

9

maximum amount of m after 128 h of ageing at 100°C is about 0.18. Also, the maximum amount of m after 128 h of aging at 250°C is about 0.2. These results are by the decrease in e_f of the aged sample for 128 h compared to the sample aged for 2 h at temperatures of 100°C and 250°C.

After 2 and 8 h of aging at 100 and 250°C, the samples show strain-softening behavior in all strain rates and with increasing aging time, both strain-softening and strain-hardening behaviors are observed. Strain-hardening behaviour is related to grain growth and dislocation stocking process during superplastic deformation [18, 20]. DRV/DRX is accepted as the strain-softening factor in superplastic materials [21]. On the other hand, a decrease in strain rate during tensile testing, if the material is strain rate sensitive, has been reported as another strain-softening factor [22]. According to these cases, the strain-softening behaviour for sub-micron grain size samples can be related to DRV/DRX. Strain-softening behaviour is more pronounced at strain rates proportional to high m (strain rates of 10^{-5} s^{-1} to 10^{-3} s^{-1} for the aged samples for 2 h at 100°C). Therefore, the change in strain rate during superplastic deformation is considered as another strain-softening factor [20]. It is known that dislocations participate in GBS as the dominant deformation mechanism and they disappear at grain boundaries that act as dislocation sinks during superplastic deformation [12]. Therefore, for samples with sub-micron grain sizes, no strain-hardening caused by dislocations is observed. For some samples with micron grain size, significant strain-hardening is observed at strain rates of 10^{-1} and 10^{-2} s^{-1}. These samples lose their superplastic behavior and sensitivity to strain rate or this sensitivity becomes less. Therefore, strain-softening occurs only by DRV/DRX due to sufficient time at low strain rates. In addition, the change in strain rate during superplastic deformation does not play a significant role [18, 20].

Strain-hardening for some samples (micron grain size) is related to the increase in dislocation density during deformation. DRX loses its effect due to insufficient time and the dislocation accumulation process occurs at high strain rates of 10^{-1} s^{-1} and 10^{-2} s^{-1} [21]. Strain-hardening in samples with micron grain size becomes more pronounced as the ageing time and strain rates increase, which is due to the change in the internal energy level with increasing ageing time [20]. The high internal energy during UFG formation is imposed by the ECAP process and this is the driving force for DRV/DRX [23]. Increasing the ageing time and generally increasing the annealing time leads to a decrease in the internal energy. Therefore, strain-hardening behaviour is not observed in the aged samples for 8 h at temperatures of 100°C and 250°C compared to aged samples for 32 and 128 h. This is because some DRV/DRX still occurs in the aged samples for 8 h due to the high internal energy level compared to the aged samples for 32 and 128 h. Therefore, the increase in the dislocation density is limited and the strain-hardening behaviour is not seen in the aged samples for 8 h at both temperatures. The results of the present study show that the increase in e_f is dependent on the grain size of Zn-22Al alloy. Decreasing the grain size of Zn-22Al alloy increases the strain rate at which the maximum superplastic elongation occurs. Since smaller grain size means more grain boundary area, GBS occurs more effectively at more boundaries, leading to higher superplastic elongation. By controlling the grain size and shape of grains, the amount of GBS can be controlled. In the present study, grain size has been studied in detail. As mentioned, whenever the grain size of the alloy decreases, the superplasticity of the alloy increases.

The effects of post-ECAP ageing on the hardness of Zn-22Al alloy are shown in Figure 12. It can be seen that the hardness curve increases with increasing ageing time and temperature compared to the sample with 8 passes of ECAP (denoted by 0 on the curve). The age-hardening behaviour becomes more pronounced when the alloy is aged at a high temperature (250°C). Correlating the hardness curve with grain size in Figure 6, it is clear that age-hardening or generally annealing-hardening is related to the coarsening of the microstructure after post-ECAP ageing. The relationships between hardness and grain size of Zn-22Al alloy after post-ECAP ageing can be seen in Figures 13 and 14. Also, the relationship between the hardness, the grain size and the ageing time are summarized in Table 2. It can be seen in Figure 12 that the application of ageing heat treatment on Zn-22Al alloy results in two sequential but completely different effects, i.e., an initial aging-hardening effect and a subsequent aging-softening effect. It should be noted that

these two separate areas are observed after ageing at 250°C. In the case of ageing at 100°C, only the aging-hardening area is visible, which can be seen in Figure 13. As seen in Figure 14, in the early stages of age-hardening, where the grain size after age-hardening is still small (less than the critical grain size, d_c), the grain coarsening heat treatment hardens the Zn-22Al alloy by reduction of heterogeneous nucleation sites of DRV/DRX [15]. This behaviour is generally observed in annealing-hardening or ageing-hardening in Figure 12, where the hardness of Zn-22Al alloy increases with increasing grain size. As grain growth continues, the amount of boundary-sensitive DRV decreases further and aging-softening begins to participate [15]. The transition from age-hardening to age-softening is quite clear in Figure 14, where the critical grain size, d_C, or the smallest grain size required to exhibit age-hardening or fine-grain softening, is about 1.6 µm. The analysis of hardness measurement results, Hv, located in the age-hardening region ($d_C \geq d$) in Figure 14 shows that the hardness data can be in the form of $H = H_0 - k_1 d^{-1}$, such as Hv$= 65.75 - 20.4 \ d^{-1}$ for Zn-22Al alloy after post-ECAP ageing at 250°C. This equation shows that the fine-grain softening behavior occurs when the grain size is less than d_C and the degree of fine-grain softening by boundary-sensitive DRV is inversely proportional to the grain size [15]. Since the grain boundary area per unit volume for spherical grains is 3/d, the amount of fine-grain softening by DRV has been proven to be linearly proportional to the grain boundary area in alloys [15]. Therefore, it can be said that when the grain size of Zn-22Al alloy is larger than the critical grain size, this alloy shows an age-softening behaviour.
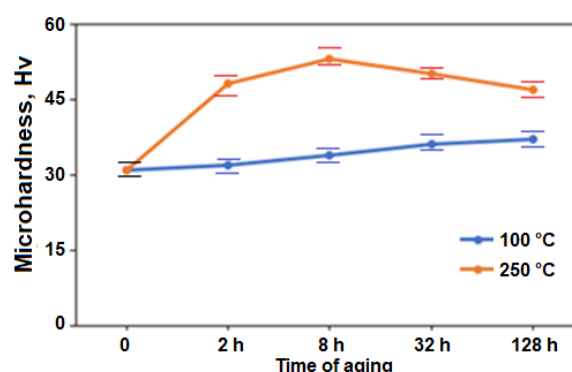

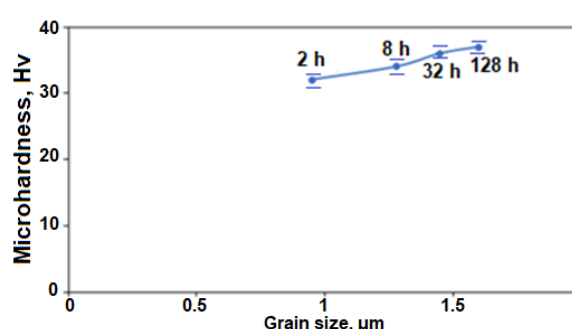**Fig. 12.** The effect of post-ECAP ageing on the hardness of Zn-22Al alloy.

Fig. 13. Relationship between the hardness and the grain size of Zn-22Al alloy after post-ECAP aging at 100°C.
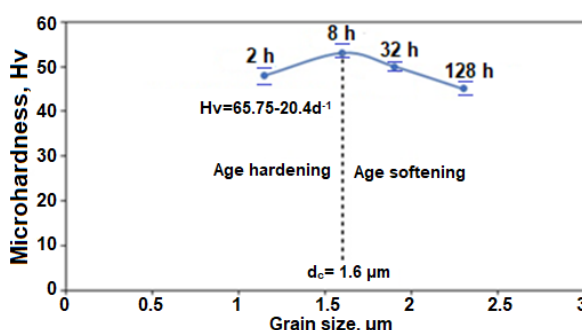

Fig. 14. Relationship between the hardness and the grain size of Zn-22Al alloy after post-ECAP ageing at 250°C.

Table 2. Relationship between the grain size, the ageing time and the hardness of Zn-22Al alloy after post-ECAP ageing.

Time of aging (h)	Grain size (µm)	Hardness (Hv)
Post-ECAP aging (100°C)		
2	0.95	32
8	1.28	34
32	1.45	36
128	1.6	37
Post-ECAP aging (250°C)		
2	1.15	48
8	1.6	53
32	1.9	50
128	2.3	45

Texture is one of the characteristics of the Zn-22Al alloy that can control the properties of UFG material. Pole figures are used for the analysis of texture evolution after post-ECAP ageing at 250°C for 128 h. Ideal orientation positions on FCC crystal components include Copper {1 1 2} <1 1 1>, S {1 2 3} <6 3 4>, Brass {0 1 1} <2 1 1>, Goss {1 1 0} <0 0 1> and Cube {0 0 1} <1 0 0> [24]. Five ideal fibres for HCP crystal are identified: B, P, Y and C_1–C_2 and correspond to a high activity of < a > type slip (B, P and Y) as well as pyramidal < c+a > (C_1-C_2) [25]. Pole figure of {111} phase α (FCC) and {0001} phase η (HCP) are shown in Figure 15. As can be seen in this figure, after post-ECAP ageing at 250°C for 128 h, the main texture in α phase is Copper {1 1 2} <1 1 1>. Also, in the η phase, P and Y components expand as the main texture. In Zn-22Al alloy, the formation of a strong crystallographic texture in both phases can lead to a relatively large increase in the e_f of the alloy. The texture intensity of α phase and η phase is 5.8 and 4.8, respectively. The results show that the preferred orientation affects the tensile behaviour of the Zn-22Al alloy and the formation of a suitable texture in the alloy leads to an increase in the e_f of the alloy. In the Zn-22Al alloy, the formation of a strong crystallographic texture in α and η phases can lead to a relatively large increase in the e_f of the alloy.

4. CONCLUSIONS

In this research, the effect of ageing on microstructure evolution and mechanical properties of Zn-22Al alloy in different situations was investigated. The most important results are as follows:

1) Based on the results of natural ageing after ECAP, it cannot be said that the microstructure of UFG Zn-22Al alloy after the ECAP process is completely stable at room temperature, but it can be said that the microstructure is quasi-stable at room temperature after ECAP process. After the natural ageing process, limited grain growth occurred. The presence of two phases in the microstructure of Zn-22Al alloy prevented the excessive growth of the phases. Also, the hardness of the naturally aged Zn-22Al alloy increased by increasing the ageing times.

2) In the post-ECAP ageing condition, more grain growth was observed with increasing ageing time or temperature. At lower times of the post-ECAP ageing process, the grain growth occurred at a faster rate. In other words, increasing ageing time decreased the rate of grain growth. The hardness value increased with increasing time and temperature of the post-ECAP ageing process.

3) It was found that after the post-ECAP aging process at a temperature of 250°C for 128 h, the main texture of α phase is Copper {1 1 2} <1 1 1>. It was demonstrated that the components of P and Y are present as the main texture of the η phase.
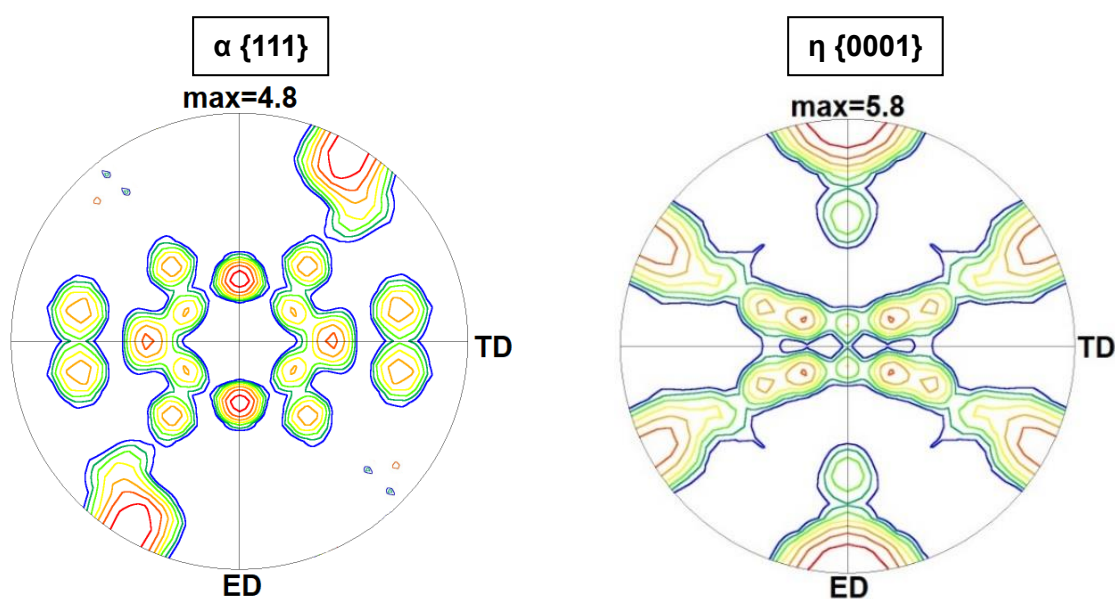

Fig. 15. Pole figures of α and η phases of Zn-22Al alloy after post-ECAP ageing process at 250°C for 128 h.

REFERENCES

[1]. Azad, B., Eivani, A. R. and Salehi, M. T., "An investigation of microstructure and mechanical properties of as-cast Zn-22Al alloy during homogenizing and equal channel angular pressing.", J. Mat. Res. Tech., 2023, 22, 3255-3269.

[2]. Demirtas, M., Pürçek, G., Yanar, H., Zhang, Z. J. and Zhang, Z. F., "Effect of Natural Aging on RT and HSR Superplasticity of Ultrafine Grained Zn-22Al Alloy.", Mater. Sci. For., 2016, 838-839, 320-325.

[3]. Tanaka, T. and Higashi, K., "Superplasticity at Room Temperature in Zn22Al Alloy Processed by Equal-Channel-Angular Extrusion.", Mater. Trans., 2004, 45, 1261-1265.

[4]. Pilling, J. and Ridley N., Superplasticity in crystalline solids, The Institute of Metals London, Brookfield, 1989, 2-83.

[5]. Engler, O., Padmanabhan, K. A. and Lücke, K., "Model for superplastic flow induced texture annihilation.", Model. Simul. Mater. Sci. Eng., 2000, 8, 477-490.

[6]. Nieh, T. G., Wadsworth, J. and Sherby, O. D., Superplasticity in Metals and Ceramics, Cambridge University Press, 1997, 22-90.

[7]. Feldner, P., Merle, B. and Göken, M., "Breakdown of the superplastic deformation behavior of heterogeneous nanomaterials at small length scales.", Mater. Res. Let., 2020, 9, 41-49.

[8]. Demirtas, M., Yanar, H. and Purcek, G., "Effect of long-term natural aging on microstructure and room temperature superplastic behavior of UFG/FG Zn-Al alloys processed by ECAP.", Let. Mater., 2018, 8, 532-537.

[9]. Tanaka, T., Chung, S.W., Chaing, L.F., Makii, K., Kushibe, A., Kohzu, M. and Higashi, K., "On applying superplastic Zn-22 wt. %Al alloy with nanocrystalline grains to general residential seismic dampers.", Mater. Sci. Eng. A., 2005, 410-411, 109-113.

[10]. Savaşkan, T. and Murphy, S., "Decomposition of Zn–Al alloys on quench–aging." Mater. Sci. Tech., 2013, 6, 695-704.

[11]. Demirtas, M., Purcek, G., Yanar, H., Zhang, Z.J. and Zhang, Z.F., "Effect of different processes on lamellar-free ultrafine grain formation, room temperature superplasticity and fracture mode of Zn-22Al alloy.", J. All. Com., 2016, 663, 775-783.

[12]. Kaibyshev, O. A., Superplasticity of Alloys Intermetallides and Ceramics, first ed., Springer- Verlag, Berlin, 1992, 19-93.

[13]. Kawasaki, M. and Langdon, T.G., "Principles of superplasticity in ultrafine-grained materials.", J. Mater. Sci., 2007, 42, 1782–1796.

[14]. Naik, S. and Walley, S. M., "The Hall–Petch and inverse Hall–Petch relations and the hardness of nanocrystalline metals.", J. Mater. Sci., 2020, 55, 2661-2681.

[15]. Yang, C., Pan, J. and Lee, T., "Work-softening and anneal-hardening behaviors in fine-grained Zn–Al alloys.", J. All. Com., 2009, 468, 230–236.

[16]. Senkov, O. N. and Myshlyaev, M. M., "Grain growth in a superplastic Zn–22% Al alloy.", Acta. Metall., 1986, 34, 97–106.

[17]. Cetin, M. E., Demirtas, M., Sofuoglu, H., Cora, Ö. N. and Purcek G., "Effects of grain size on room temperature deformation behavior of Zn–22Al alloy under uniaxial and biaxial loading conditions.", Mater. Sci. Eng. A., 2016, 672, 78–87.

[18]. Abbaschian R., Abbaschian, L. and Reed-Hill, R. E., Physical Metallurgy Principles, 4th ed., Cengage Learning, USA, 2009, 55-202.

[19]. Demirtas, M., Purcek, G., Yanar, H., Zhang, Z. J. and Zhang, Z. F., "Effect of equal-channel angular pressing on room temperature superplasticity of quasi-single phase Zn–0.3Al alloy.", Mater. Sci. Eng. A., 2015, 644, 17, 17-24.

[20]. Mohammadi, H., Eivani, A. R., Seyedein, S. H., Ghosh, M. and Jafarian, H. R., "Evolution of dynamic recrystallization behavior and simulation of isothermal compression of Zn–22Al alloy.", J. Mater. Res. Tech., 2023, 24, 4009-4023.

[21]. Wei, Y. H., Wang, Q. D., Zhu, P., Zhou, H. T., Ding, W. J., Chino, Y. and Mabuchi, M., "Superplasticity and grain boundary sliding in rolled AZ91 magnesium alloy at high strain rates." Mater. Sci. Eng. A.,

2003, 360, 107-115.

[22]. Mcnelley, T.R., Lee, E.W. and Mills, M.E., "Superplasticity in a thermomechanically processed high–Mg, AI–Mg alloy.", Metall. Trans. A., 1986, 17, 1035–1041.

[23]. Waitz, T., Kazykhanov, V. and Karnthaler, H. P., "Microstructure and Phase Transformations of HPT NiTi." in: M. J. Zehetbauer, R. Z. Valiev (Eds.), Nanomaterials by Severe Plastic Deformation, VCHWiley Weinheim, Germany, 2004, 351-356.

[24]. Azad, B. and Borhani, E., "Pre-Aging Time Dependence of Microstructure and Mechanical Properties in Nanostructured Al-2wt%Cu Alloy.", Met. Mater. Int., 2016, 22, 243-251.

[25]. Beausir, B., Toth, L S. and Neale, K. W., "Ideal orientations and persistence characteristics of hexagonal close packed crystals in simple shear." Acta. Mater., 2007, 55, 2695–2705.